Marine Environmental Research 179 (2022) 105693

Contents lists available at ScienceDirect

Marine Environmental Research

journal homepage: www.elsevier.com/locate/marenvrev

The effect of short-term temperature exposure on vital physiological processes of mixoplankton and protozooplankton

Guilherme D. Ferreira [a,b,1], Afroditi Grigoropoulou [a,2,3], Enric Saiz [a], Albert Calbet [a,*]

[a] Institut de Ciències del Mar, CSIC, Pg. Marítim de la Barceloneta, 37-49, 08003 Barcelona, Spain
[b] Marine Biological Section, University of Copenhagen, DK-3000, Helsingør, Denmark

ARTICLE INFO

Keywords:
Temperature acclimation
Protist
Mixoplankton
Mixotrophy
Grazing
Growth

ABSTRACT

Sudden environmental changes like marine heatwaves will become more intense and frequent in the future. Understanding the physiological responses of mixoplankton and protozooplankton, key members of marine food webs, to temperature is crucial. Here, we studied two dinoflagellates (one protozoo- and one mixoplanktonic), two ciliates (one protozoo- and one mixoplanktonic), and two cryptophytes. We report the acute (24 h) responses on growth and grazing to a range of temperatures (5–34 °C). We also determined respiration and photosynthetic rates for the four grazers within 6 °C of warming. The thermal performance curves showed that, in general, ciliates have higher optimal temperatures than dinoflagellates and that protozooplankton is better adapted to warming than mixoplankton. Our results confirmed that warmer temperatures decrease the cellular volumes of all species. Q_{10} coefficients suggest that grazing is the rate that increases the most in response to temperature in protozooplankton. Yet, in mixoplankton, grazing decreased in warmer temperatures, whereas photosynthesis increased. Therefore, we suggest that the Metabolic Theory of Ecology should reassess mixoplankton's position for the correct parameterisation of future climate change models. Future studies should also address the multigenerational response to temperature changes, to confirm whether mixoplankton become more phototrophic than phagotrophic in a warming scenario after adaptation.

1. Introduction

Climate change is expected to affect marine ecosystems and their biodiversity profoundly. One of the major issues surrounding this topic is the prediction that sea surface temperatures will rise continually (e.g., Xiao et al., 2019). In this regard, higher temperatures are predicted to increase both autotrophic and heterotrophic processes (such as photosynthesis and ingestion, respectively), albeit at different rates (e.g., Regaudie-de-Gioux and Duarte, 2012). In particular, the Metabolic Theory of Ecology (MTE – Brown et al., 2004) predicts that the activation energy (*Ea*) for the rate-limiting biochemical reactions of photosynthesis is significantly lower than the value for heterotrophic activities such as respiration and grazing (Regaudie-de-Gioux and Duarte, 2012; Rose and Caron, 2007). Therefore, in a warming scenario, marine ecosystems are expected to become less efficient at capturing carbon from the atmosphere, due to the prevalence of heterotrophic processes over autotrophic ones, at least over short time scales (Barton et al., 2020).

Still, this prediction is based on organisms that expressed either exclusive heterotrophy or autotrophy and did not consider photo-phago-mixotrophy. The term mixoplankton has been recently coined to designate photo-phagotrophic protists (Flynn et al., 2019) and will be used throughout this work (exclusive phago-heterotrophs will be referred to as protozooplankton, and exclusive photo-autotrophs as phytoplankton). If we apply the MTE prediction as a universal law, we could also assume that, in mixoplankton, heterotrophic processes are expected to increase faster than autotrophic ones in response to warmer temperatures. This would shift the balance of photo/phagotrophy towards the latter mode of nutrition in mixoplankton.

It is important to mention that, irrespective of the trophic mode of nutrition, a change in metabolic rates due to temperature is going to repercuss on the performance of the individual, and thence on the population, and ultimately, on the entire ecosystem (Hochachka and

* Corresponding author.
E-mail address: acalbet@icm.csic.es (A. Calbet).
[1] Current address: ESTM, Polytechnic of Leiria, 2520-630 Peniche, Portugal
[2] Current address: Leibniz Institute of Freshwater Ecology and Inland Fisheries, Department of Ecosystem Research, Müggelseedamm 310, 12587 Berlin, Germany
[3] Current address: Freie Universität Berlin, Department of Biology, Chemistry, Pharmacy, Institute of Biology, Königin-Luise-Str. 1-3, 14195 Berlin, Germany

https://doi.org/10.1016/j.marenvres.2022.105693
Received 2 March 2022; Received in revised form 16 June 2022; Accepted 21 June 2022
Available online 26 June 2022

Somero, 2002). Furthermore, the temperature may also directly affect vertical and/or latitudinal distributions of organisms (Angilletta Jr and Angilletta, 2009), which could be a source of unexpected biological interactions through predation or competition and affect the species composition of a given ecosystem (Montagnes et al., 2008). In addition, a direct consequence of climate change (yet understudied) is an increased frequency and intensity of extreme short-term events (Salles et al., 2016) such as marine heatwaves, which are responsible for a sudden temperature change (Oliver et al., 2019). Experimenting on the ecosystem is unrealistic due to time and scale constraints because changes require longer periods of time to be noticeable, and sample representability is hard to determine. Thus, the best way to predict how will the ecosystem respond to a given stressor (such as temperature) is to experiment on a low organisational level, whose changes are likely going to affect the ecosystem (Lemos et al., 2010).

Therefore, measuring key metabolic rates on a diverse group of organisms within the ecosystem seems to be the ideal approach to study large ecosystem processes like the effects of temperature shifts. The visualisation of these effects requires the assembling of a thermal performance curve (Angilletta Jr and Angilletta, 2009; Schulte et al., 2011) These curves are extremely useful in predicting the responses of populations to climate change, namely due to their possible incorporation into mechanistic models (Angert et al., 2011). Given the recent acknowledgement of the widespread occurrence of mixoplankton in microbial food webs, determining their thermal performance curves may promote an accurate integration into biogeochemical models (Mitra et al., 2014). Nevertheless, at the moment, data on the effects of temperature on key physiological parameters of mixoplankton are relatively scarce and contradictory (Cabrerizo et al., 2019; González-Olalla et al., 2019; Princiotta et al., 2016; Wilken et al., 2013).

Therefore, in this study, we aimed to determine the short-term (ca. 24 h) thermal performance curves for some phyto-, protozoo-, and mixoplanktonic species. We also measured respiration and photosynthetic rates on the phagotrophic species over a shorter temperature range to understand how temperature changes affect the internal metabolism of protozoo- and mixoplanktonic species. Altogether, the data collected with our experiments may, in future, fuel climate change models while attempting to clarify the place of mixoplankton within the MTE (either as enhanced producers or consumers in the ecosystem i.e., increased autotrophy or phagotrophy).

2. Methods

2.1. Cultures

We conducted the experiments with two protozooplankton species: the dinoflagellate *Gyrodinium dominans* (strain ICM-ZOO-GD001), and the ciliate *Strombidium arenicola* (strain ICM-ZOO-SA001). We also used two mixoplanktonic species from distinct functional groups (Mitra et al., 2016): the constitutive dinoflagellate *Karlodinium armiger* (strain ICM-ZOO-KA001), and the plastidic-specialist ciliate *Mesodinium rubrum* (strain DK-2009). The two dinoflagellates and the ciliate *S. arenicola* were fed the cryptophyte *Rhodomonas salina ad libitum* during the up-scale period. To avoid the depletion of *R. salina* in the predator's cultures, we supplied them with fresh cryptophytes every second or third day, depending on the predator species. *M. rubrum* was offered the cryptophyte *Teleaulax amphioxeia* (strain K-1837) as prey in a proportion of ca. 1:5 (Smith and Hansen, 2007) during the up-scaling process. Protozooplankton and mixoplankton were maintained at ca. 100 μmol photons m^{-2} s^{-1}, in autoclaved 0.1-μm filtered seawater. Both cryptophytes were grown in f/2 medium (Guillard, 1975), prepared using autoclaved 0.1-μm filtered seawater, and irradiated at ca. 150 μmol photons m^{-2} s^{-1} provided by cool white fluorescent lights. To maintain the organisms under exponential growth (and within target concentrations), the stock cultures were diluted every 1–2 days with fresh medium (between 20 and 50% of the total volume). All cultures were kept at a salinity of 38 in a temperature-controlled room at 19 °C with a 10:14 L/D cycle.

2.2. Cell counts and volumes

Except for *M. rubrum* and its prey, all the organisms were counted and sized with a Beckman Coulter Multisizer III particle counter. *M. rubrum* may escape the current flow generated by the particle counter due to their sensitivity to shear and fast jump responses (Ferreira and Calbet, 2020). Therefore, cell counts of this ciliate using this instrument are often not representative of the concentration of the entire population. Accordingly, aliquots of *M. rubrum,* fixed in acidic Lugol's solution (final concentration 2%), were prepared for all the treatments. A minimum of 300 predator and prey cells were counted using a Sedgwick-Rafter counting chamber. Additionally, 30 organisms were sized per replicate using the Fiji software (Schindelin et al., 2012); i.e., 90 cells were measured per temperature for the feeding and respiration experiments. Organismal volumes were estimated from linear dimensions using the following geometric shapes: for *M. rubrum*, a rotational ellipsoid, and for *T. amphioxeia*, the added volume of a hemisphere and a cone (Smith and Hansen, 2007).

Since we noticed that *M. rubrum* and *T. amphioxeia* cells enlarged when fixed in Lugol's solution (using the previously described geometrical models), we conducted an independent trial where we sampled a single population of each species (for *M. rubrum*, $n > 1.0 \times 10^3$ cells; for *T. amphioxeia*, $n > 1.3 \times 10^6$ cells) and ran an aliquot through the Beckman Coulter Multisizer III while fixing another in acidic Lugol's (final concentration 2%). Despite not rendering trustable cell counts for *M. rubrum*, the electronic particle counter provided accurate volume estimations. We measured 200 organisms of each species from the fixed sample and obtained a conversion factor to correct the Lugol's-preserved volumes (μm^3) into live volumes (μm^3) using the organisms measured with the electronic particle counter. For *M. rubrum*, Live Volume = 0.336 × Lugol Volume +1169.443; for *T. amphioxeia* Live Volume = 0.456 × Lugol Volume – 1.229 (Figs. S1 and S2 of the Supplementary Information).

Irrespective of the species, the changes in cellular volume (ΔVolume, μm^3) were used to assess the effect of temperature and were calculated according to Equation 1

$$\text{Volume}_{Temp} = \text{V}f_{Temp} - \text{V}i_{Temp} \quad (1)$$

where V*f* corresponds to the average volume of a cell (μm^3) within a population after being exposed to a given target temperature (*Temp*, °C) for ca. 24 h. V*i*, on the other hand, depicts the average volume of a cell (μm^3) before exposure to the target temperature. Carbon values for all species were obtained from the pg C:μm^3 ratio provided by Traboni et al. (2020) and used to determine C-specific rates.

2.3. Thermal performance curves

To assess the acute effects of temperature on the growth and grazing rates of protozooplanktonic and mixoplanktonic grazers, we exposed them to a wide range of temperatures (5–34 °C) for ca. 24 h with a 10:14 L/D regime at 100 μmol photons m^{-2} s^{-1}. These temperatures were reached and maintained using recirculating water baths connected to individual aquarium chillers and heaters (TECO®). The incubations were conducted in triplicate experimental (predator and prey) and control (only prey) 132 mL Pyrex bottles. The bottles were submerged in the water baths during the incubation, and the temperature was monitored continuously using an Onset HOBO data logger. The target temperature was always reached within 20 min (from the initial stock temperature of 19 °C). Thermal performance curves of the growth rates of the cryptophytes *R. salina* and *T. amphioxeia*, used as prey in the incubations, were obtained from the control bottles in the grazing experiments.

The experimental and control suspensions were prepared with the addition of 100 mL of fresh f/2 medium per L of suspension (final nutrient concentration equivalent to f/20 medium – Guillard, 1975). The objective was to avoid nutrient limitation for the prey during the incubation. During these experiments, *K. armiger*, *G. dominans,* and *S. arenicola* were fed *R. salina*, whereas *M. rubrum* was fed *T. amphioxeia*. All the experiments were conducted at saturating food concentrations (Table 1) to minimise the effect of different food concentrations on the measured ingestion rates. Predator concentrations were adjusted to allow ca. 30% of the prey to be consumed during the incubation while maintaining saturating food conditions.

All bottles were filled gradually, in three or four steps, using the corresponding experimental and/or control suspension, which was carefully mixed in between fillings. Additional experimental and control bottles were sacrificed at the beginning of the incubations to obtain the initial concentrations of the organisms. Cell numbers and volumes were obtained as described before. Growth and grazing rates at each target temperature were calculated after ca. 24 h of incubation using Frost (1972) and Heinbokel (1978) equations. Ingestion rates were deemed significant (i.e., not 0) only when the control and experimental bottles' prey growth rates differed significantly (two-tailed Student's t-test, $P < 0.05$). The temperature at which a given rate was maximised was termed T_{opt} and the range of temperatures where this rate's performance met or exceeded 80% of the observed at T_{opt} was defined as $T_{breadth}$ (Schulte et al., 2011).

2.4. Oxygen consumption and production rates

In addition to the feeding experiments, we conducted parallel trials at three different temperatures to quantify the consumption and production rates of oxygen during light and dark conditions. The chosen temperatures included the one used for the maintenance of parental cultures (i.e., 19 °C), and 3 °C below and above it. We used optical oxygen sensors (OxygenDipping Probe DP-PSt3, PresensH) at the beginning and at the end of the incubations (that lasted ca. 24 h) to determine oxygen concentrations. These experiments were conducted in triplicate experimental and control bottles, under a regular diel light cycle (light bottles; i.e., with a 10:14 L/D regime, 100 μmol photons m^{-2} s^{-1}) or wrapped in aluminium foil throughout the incubation (dark bottles; i.e., with no light through the whole incubation). The control bottles contained only 0.1 μm-filtered seawater, whereas the experimental ones also contained grazers at a known concentration. The prey concentrations in the predator stock cultures were adjusted to guarantee their depletion on the night before the experiment, and therefore ensure a good physiological condition of the predators while eliminating the possible artefacts that co-existing prey could induce (Almeda et al., 2011; Calbet et al., 2022). Nevertheless, the absence of prey was further confirmed before the beginning of the experiments with the aid of the electronic particle counter. Additionally, initial bottles were also prepared in triplicate to assess the initial oxygen concentrations, necessary to compute the oxygen consumption rates later.

The oxygen consumption rates under darkness (O_{Dark}, μmol O_2 L^{-1} h^{-1}) were obtained considering triplicate dark bottles (i.e., ca. 24 h of darkness) using Equation (2) to determine the oxygen consumption of each individual dark bottle

$$O_{Dark} = \left(\frac{\overline{Ctr_f} - \overline{Ctr_i}}{\overline{t_{Ctr}}}\right) - \left(\frac{Exp_f - \overline{Exp_i}}{t_{Exp}}\right) \quad (2)$$

where *Ctr* corresponds to the oxygen concentration (μmol O_2 L^{-1}) inside the control bottles and Exp to the same parameter inside experimental bottles, and the subindex *f* and *i* correspond to the final and initial values, respectively. The incubation time (h) for the experimental bottles is represented by t_{Exp} and for the control bottles by t_{Ctr}. The horizontal bars above some parcels of the equation (e.g., $\overline{Exp_i}$) indicate that the average of the three replicates should be used.

The oxygen consumption rates obtained using Equation (2) were converted into per *capita* rates by dividing O_{Dark} by the average cell concentration of grazers in each bottle. These concentrations were obtained using Frost (1972) and Heinbokel (1978) equations after measuring the initial and final concentration of organisms as described before. Finally, oxygen consumption rates (under darkness) per unit of carbon per hour (i.e., respiration rates, *R*, μmol O_2 pg C^{-1} h^{-1}) were obtained from the division of the last value by the average C concentration (pg C L^{-1}) in the same bottle, which was calculated from the C:μ m^3 ratio provided by Traboni et al. (2020). Notice that the calculation of *R* as described yields a positive value even though it is a C loss for the organism.

We considered only the triplicate light bottles to calculate oxygen consumption/production rates during the light period (O_{Light}, μmol O_2 L^{-1} h^{-1}) for both mixoplanktonic and protozooplanktonic grazers. We assumed that the respiration rate *R* was the same in the dark and light bottles (Wielgat-Rychert et al., 2017) and considered that our experimental setup for the latter comprised 14 h of darkness (as per the L/D cycle of the culture room). Equation (3) was then applied

$$O_{Light} = \frac{\left[\left(\frac{\left[Exp_f + \left(\overline{R} \times C_{Exp} \times 14\right)\right] - \overline{Exp_i}}{t_{Exp}}\right) - \left(\frac{\overline{Ctr_f} - \overline{Ctr_i}}{\overline{t_{Ctr}}}\right)\right] \times t_{Exp}}{t_{Exp} - 14} \quad (3)$$

where *Exp*, *Ctr*, t_{Exp}, t_{Ctr}, and the letters *f* and *i* have the same meaning as in Equation (2). The horizontal bars above specific parcels, as in Equation (2), also indicate average values. *R* is the respiration rate (μmol O_2 pg C^{-1} h^{-1}) as calculated before from the dark bottles, and C_{Exp} is the average concentration of C in the experimental bottle (from the grazer), as calculated using Frost (1972) equations. Per *capita* and per unit of carbon values were obtained as described before.

For mixoplanktonic species, $O_{Dark} = R$ and $O_{Light} = P$ (photosynthetic rate), according to Wielgat-Rychert et al. (2017). For protozooplankton, O_{Light} resulted in negative values, i.e., oxygen consumption during the hours of light and, therefore, light bottles were considered replicates from the dark incubations, and their average was used to determine *R* in protozooplankton (i.e., $\overline{O_{Light}:O_{Dark}} = R$).

For the C-specific respiration (C losses), we multiplied *R* by the average respiratory quotient (moles of carbon dioxide produced per mole of oxygen consumed) of 0.89 (Williams and del Giorgio, 2005). The exact opposite, i.e., the molar ratio of oxygen produced to fixed carbon dioxide via photosynthesis, is called the photosynthetic quotient. Likewise, we multiplied *P* by the average photosynthetic quotient of 1.28 (Wielgat-Rychert et al., 2017) to obtain C-specific photosynthetic rates.

Table 1
Summary of the prey and predator concentrations used for the assembling of the thermal performance curves for the predator species, the protozooplanktonic *G. dominans* and *S. arenicola*, and the mixoplanktonic *K. armiger* and *M. rubrum*. All concentrations were based on published functional responses.

Species	Target concentration, Cells mL^{-1}		Functional Response
	Prey	Predator	
Gyrodinium dominans	100,000	1500	Calbet et al. (2013)
Strombidium arenicola	100,000	400	Ferreira et al. (2021)
Karlodinium armiger	100,000	3750	Berge et al. (2008)
Mesodinium rubrum	15,000	1500	Smith and Hansen (2007)

2.5. Activation energies and Q_{10} coefficients

Activation energies (*Ea*, given in eV) can be obtained from the slope of the linear regression between the natural logarithm of a given rate versus the inverse of the absolute temperature (given in Kelvin, K) multiplied by the Boltzmann's constant (8.62×10^{-5} eV K^{-1}) (Vaquer-Sunyer et al., 2010). This plot is commonly referred to as an

Arrhenius plot. Therefore, each physiological rate yields an individual Arrhenius plot for each species. To make it easier for the reader, we decided to convert *Ea* into Q_{10} coefficients, which represent the fold-increase in a given rate within a 10 °C variation, using Equation (4) (Vaquer-Sunyer et al., 2010)

$$Q_{10} = e^{\left(\frac{10Ea}{RT^2}\right)} \quad (4)$$

where R is the gas constant (8.314 J mol^{-1} K^{-1}), and T is the mean absolute temperature for the range over which Q_{10} was measured (upper and lower thermal extremes excluded – e.g., Eppley, 1972). For this calculation, *Ea* were expressed in J mol^{-1} using a conversion factor of 96486.9 (Vaquer-Sunyer et al., 2010).

3. Results

3.1. Temperature effects on tolerance and performance

The C-specific thermal performance curves for all six species are shown in Fig. 1 (for cell-specific rates, the reader is referred to Fig. S3), and the respective T_{opt} and $T_{breadth}$ are shown in Table 2. All species displayed a thermal performance curve characterised by a gradual increase up to T_{opt} followed by a sharp decline for both C-specific growth and grazing rates.

Table 2
Summary of T_{opt} and $T_{breadth}$ (°C) for each species obtained from the species-specific thermal performance curves displayed in Fig. 1. NA = not applicable.

Species	T_{opt} Growth	$T_{breadth}$ Growth	T_{opt} Grazing	$T_{breadth}$ Grazing
Rhodomonas salina	25.07	10.61	NA	NA
Teleaulax amphioxeia	21.90	5.99	NA	NA
Gyrodinium dominans	25.74	8.63	22.62	7.67
Strombidium arenicola	32.52	11.05	30.49	9.71
Karlodinium armiger	16.01	11.39	16.01	14.65
Mesodinium rubrum	21.90	7.22	19.08	6.06

The C-specific thermal performance curves for growth of the cryptophytes *R. salina* and *T. amphioxeia* are displayed in Fig. 1a and b, respectively. The former exhibited a higher T_{opt} and $T_{breadth}$ than the latter and showed positive C-specific growth rate in a wider temperature range as well (ca. 5.3–31.1 °C for *R. salina*, as opposed to 7.3–25.9 °C for *T. amphioxeia*). Among all species studied (prey or predator),

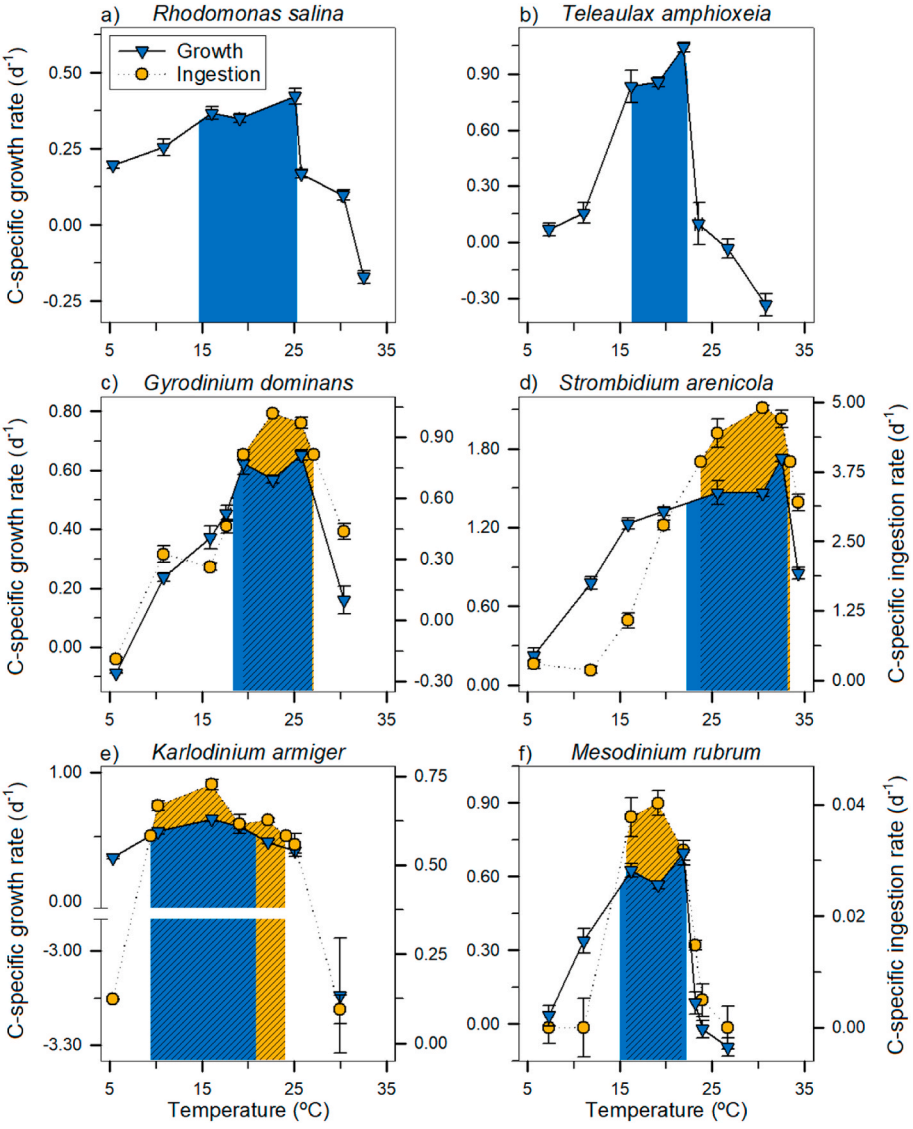

Fig. 1. C-specific thermal performance curves for the studied protists in terms of growth (inverted blue triangles) and ingestion (yellow circles): a and b) the phytoplankton *R. salina* and *T. amphioxeia*; c and d) the protozooplankton *G. dominans* and *S. arenicola*; e and f) the mixoplankton *K. armiger* and *M. rubrum*. The shaded areas limit the $T_{breadth}$ for each rate. *M. rubrum* exhibited non-significant ingestion rates at some temperatures (two-tailed Student's t-test, $P > 0.05$). The negative ingestion rates in *G. dominans* were significant (two-tailed Student's t-test, $P < 0.05$) and, therefore, shown. Error bars ± se.

T. amphioxeia was the species with the narrowest $T_{breadth}$ (Table 2). Indeed, this cryptophyte could only grow at rates up to 80% of the maximum rate between 16.3 and 22.3 °C.

The thermal performance curves of the two protozooplankters can be found in Fig. 1c (*G. dominans*) and **1d** (*S. arenicola*). These organisms tolerated wide variations in temperature, as seen by the range of temperatures exhibiting positive growth rates. For the dinoflagellate *G. dominans* the survivability range broadened over ca. 23.6 °C difference (Fig. 1c). *G. dominans* was the only species showing significantly negative ingestion rates ($P < 0.05$ at ca. 5.6 °C), which were paired with negative growth rates. For the ciliate *S. arenicola*, positive growth rates were detected on all temperatures tested (5.6–34.4 °C – Fig. 1d). In addition, *S. arenicola* also showed the highest T_{opt} for both rates across all species (ca. 32.5 °C and 30.5 °C for growth and grazing, respectively – Table 2).

Regarding mixoplankton (Fig. 1e and f), *K. armiger* showed a wide thermal performance curve, with the characteristic sharp decrease occurring ca. 9 °C above the T_{opt}, whereas for the remaining species it occurred always within 2 °C. The widening of *K. armiger*'s curve resulted in the largest $T_{breadth}$ among all species, both in terms of growth and grazing rates (Table 2). Conversely, among the four predators, *M. rubrum* was the one displaying the narrowest $T_{breadth}$, both in terms of growth and grazing rates (Table 2). In addition, the mixoplanktonic ciliate was the most sensitive species in our study, as its survivability range was narrower than in any other species (ca. 16.5 °C, between 7.3 and 23.8 °C). Finally, *K. armiger* showed the lowest T_{opt} and was the only species whose T_{opt} was lower than the maintenance temperature (ca. 19 °C) to which all species were exposed before the experiment.

3.2. Temperature effects on cellular volumes

The thermal performance curves also enabled the assessment of the overall effect of temperature on the ΔVolume (see the Methods section for the calculation procedure) of each target species (Fig. 2). All species showed a significant decrease in cellular volume ($P < 0.01$ in all instances) at higher temperatures, being this effect more evident in the predators than in the cryptophytes, as noticed by the higher correlation coefficients.

We also applied simple linear regression models between ΔVolume and C-specific growth rates (Fig. 3), and between C-specific ingestion rates and ΔVolume (Fig. 4). For *R. salina* the regression between ΔVolume and C-specific growth was not significant ($P = 0.09$ – Fig. 3a). Conversely, *T. amphioxeia* displayed a significantly negative regression between ΔVolume and C-specific growth rates (Fig. 3b). The same pattern was observed in the ciliate *S. arenicola* (Fig. 3d), with the addition that ΔVolume was also negatively associated with ingestion rates (Fig. 4b). For both *G. dominans* and *M. rubrum*, the variation in volume was positively correlated with growth (Fig. 3c,f – $P < 0.01$); however, ingestion rates could not explain the variation in volume for both species (Fig. 4a,d – $P > 0.05$). Finally, *K. armiger* exhibited a unique pattern: the ΔVolume explained ca. 63% of the observed changes in C-specific growth rates (Fig. 3e) and was itself highly dependent on the measured C-specific ingestion (Fig. 4c).

3.3. Temperature effects on physiological rates

C-specific respiration rates of both protozooplanktonic grazers showed a significant increase ($P < 0.01$) in respiratory rates as temperature rose (Fig. 5a and b), whereas mixoplanktonic grazers seemed unaffected (Fig. 5c and d). For the ciliate *M. rubrum*, photosynthesis was also unaffected by temperature ($P > 0.05$ – Fig. 5d). However, *K. armiger* nearly doubled its C-specific photosynthetic rates (from ca. 0.41 d^{-1} to ca. 0.78 d^{-1}, $P < 0.01$ – Fig. 5c) from 16.2 to 21.9 °C. Ciliates showed higher C-specific rates than dinoflagellates within a given trophic mode of nutrition. Altogether, this information resulted in distinct overall responses to temperature, as summarized by the rate-specific Q_{10} coefficients (Table 3). The respective Arrhenius plots and *Ea* can be found in Fig. S4 and Table S1 respectively.

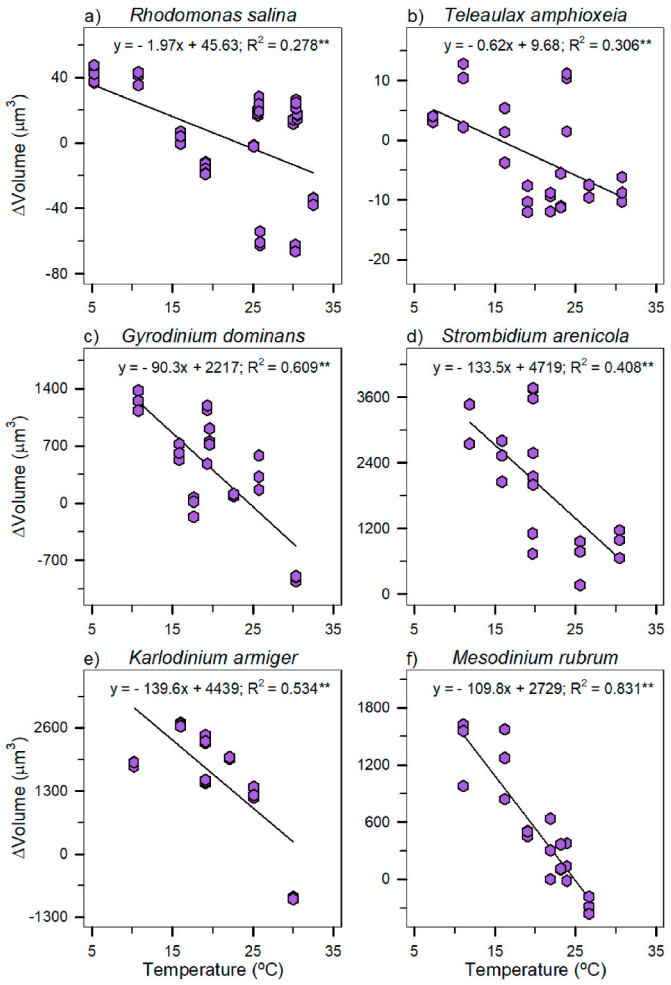

Fig. 2. Relationship between temperature (°C) and changes in volume (μm^3, relative to the initial volume at 19 °C, i.e., before exposure) for a) *R. salina*, b) *T. amphioxeia*, c) *G. dominans*, d) *S. arenicola*, e) *K. armiger*, and f) *M. rubrum*. All relationships yielded significant negative slopes (** implies $P < 0.01$). The results for *R. salina* and *T. amphioxeia* were obtained from the bottles without predators.

The Q_{10} coefficients calculated for growth and grazing rates were consistently higher in protozooplankton than in mixoplankton, irrespective of the species. In fact, growth and grazing rates displayed a $Q_{10} < 1$ for both mixoplanktonic predators, as opposed to an average Q_{10} of 1.68 and 2.88 for growth and grazing, respectively, in the protozooplanktonic grazers. In addition, the Q_{10} coefficients for grazing were the ones with the highest difference between trophic modes, being ca. 5.6 times higher in protozooplankton than in mixoplankton. Conversely, photosynthesis was the physiological process that varied the most in mixoplankton in response to temperature changes, with *K. armiger* exhibiting the highest fold increase (ca. 1.91 vs ca. 1.05 in *M. rubrum*). Regarding respiration rates, the two protozooplankters displayed a higher sensitivity to temperature than their mixoplanktonic counterparts, by exhibiting an average Q_{10} of 1.76, compared to 1.15 in mixoplankton.

4. Discussion

The objective of this research was to assess the short-term physiological response of protists to a sudden variation in temperature. In this regard, our study evidenced that several key physiological parameters

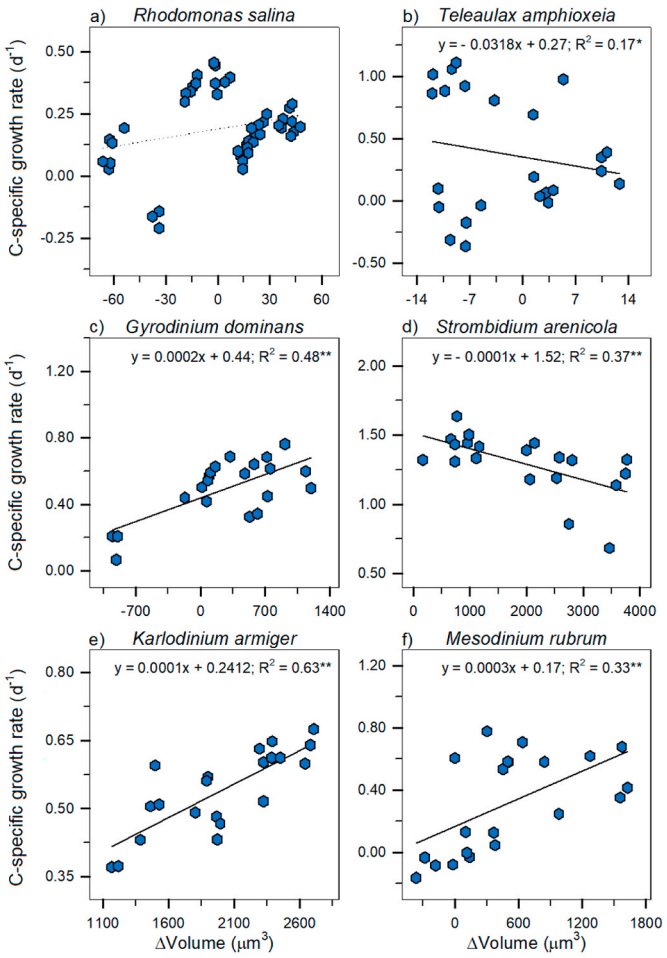

Fig. 3. Linear regression models between changes in predator's volumes (μm^3) and C-specific growth rates. Non-significant regressions ($P > 0.05$) are depicted with a dotted line, whereas significant regressions are displayed with a solid line (* implies $P < 0.05$; ** implies $P < 0.01$).

are heavily modulated by temperature (Figs. 1 and 5), with grazing and photosynthesis being the highest temperature-dependent parameters in protozooplankton and mixoplankton, respectively (Table 3). In addition, we observed that higher temperatures implied smaller organisms (Fig. 2). The lack of an acclimation period is not a very common approach in studies aiming to determine the physiological consequences of temperature changes (Kang et al., 2020; Lim et al., 2019; Ok et al., 2019). Still, there are studies where metabolic responses have been directly measured after an acclimation period of 15 min (e.g., Padfield et al., 2016). The rationale behind our experimental design was to improve the similarities between our laboratory experiment and an extreme short-term temperature event in the field, such as marine heatwaves (whose frequency and intensity are projected to increase in the future – (Oliver et al., 2019), water mass displacements, etc. Therefore, our data intend to address a specific question, and we must highlight that different time scales allow different processes to occur, which could imply different effects. Indeed, Franzè and Menden-Deuer (2020) state that physiological acclimation can take up to 2.5 d $°C^{-1}$ when transitioning towards lower temperatures and 1.25 d $°C^{-1}$ when temperatures increase. Thus, our experiments may have slightly overestimated the variations of the measured rates in response to temperature (compared to more extensive time-scale studies). However, these differences were likely minor (as per the differences in non-acclimated vs acclimated populations (Franzé and Menden-Deuer, 2020; pers. obs.). Moreover, given the fast generation times of the species studied (Fig. S3), only ≤24 h experiments can capture the individual physiological response to temperature.

4.1. Temperature effects on thermal tolerance and performance

K. armiger showed a particularly wide $T_{breadth}$ in growth and ingestion rates (Fig. 1e and Table 2). It is not the first time a similar response is seen, as exemplified by its congener *Karlodinium veneficum* (Lin et al., 2018; Vidyarathna et al., 2020) and by other mixoplanktonic dinoflagellates (Kang et al., 2020; Lim et al., 2019; Ok et al., 2019). These wide $T_{breadths}$ could be the reason why these dinoflagellates possess a global distribution (Leles et al., 2019), as it would provide them with the necessary traits to colonise different environments characterised by variable temperatures (Angilletta Jr and Angilletta, 2009). The opposite (i.e., a narrow $T_{breadth}$) was found in the ciliate *M. rubrum* and the cryptophyte *T. amphioxeia* (Fig. 1b,f and Table 2). In the work of Fiorendino et al. (2020) the $T_{breadths}$ for these two species were similar to those obtained in our study; however, T_{opts} were slightly higher than ours even though the strains used were the same. Still, in the work of Fiorendino et al. (2020) both species were adapted to a slightly higher temperature than in our experiments and they were acclimated for 2 days for every °C of variation until the experimental temperature was reached. Thus, this procedure may have increased their tolerance and performance to higher temperatures (Chakravarti et al., 2017). Gaillard et al. (2020) found similar growth performances for *T. amphioxeia* in response to temperature. Thus, the combined assessment of our and other studies suggests that *M. rubrum* and its prey are tightly coupled in terms of thermal tolerance.

In addition, we have also confirmed that for the species investigated, protozooplanktonic predators are better adapted to a sudden increase of temperature than their mixoplanktonic counterparts, as seen by the higher average T_{opts} (both in growth and ingestion rates) in the former group (Table 2). Regarding protozooplankton, we must highlight the negative ingestion and growth rates obtained at the lowest temperature in *G. dominans*' performance curve (Fig. 1c). These results denote a higher growth of the prey in the presence of the dinoflagellate than when incubated alone (controls), and likely resulted from an increase in the nutrient pool because of the death of grazers (e.g., Ferreira and Calbet, 2020). We attempted to eliminate this possible artefact by adding nutrients to the experimental suspensions; however, ammonium and urea, for example, can be released by dead microplankton (Caperon et al., 1979; Gao et al., 2018) and may explain the increased growth of *R. salina*. Franzè and Menden-Deuer (2020) previously reported mortality at similar temperatures, which could suggest that there is a threshold temperature for *G. dominans* around 5–6 °C. Finally, our results also indicate that the *R. salina* strain used in this study was better adapted to varying water temperatures than the one studied by Hammer et al. (2002), as seen by the better performance displayed at all temperatures.

4.2. Temperature effects on cellular volumes

Volume reductions due to temperature increases have been observed previously (Franzè and Menden-Deuer, 2020; Montagnes et al., 2008), and it has been proposed as a universal ecological response to increasing ambient temperatures (Daufresne et al., 2009; Sheridan and Bickford, 2011). Reductions in cell volume could be a consequence of individual cell shrinkage or higher cellular division rates. In addition, in the case of the grazers, changes in volume can also be a consequence of the ingestion of prey. Volume reductions have also physiological consequences. For instance, nutrient acquisition in phototrophs depends on the cellular surface/volume relationship (Pasciak and Gavis, 1974). Likewise, ingestion rates for planktonic grazers depend heavily on prey encounter rates, which is also a function of cell size (Kiørboe and MacKenzie, 1995). Our study demonstrated that the ciliate *S. arenicola* exhibited a significantly negative slope of the linear regressions between C-specific ingestion and ΔVolume, and ΔVolume and C-specific growth (Figs. 3d

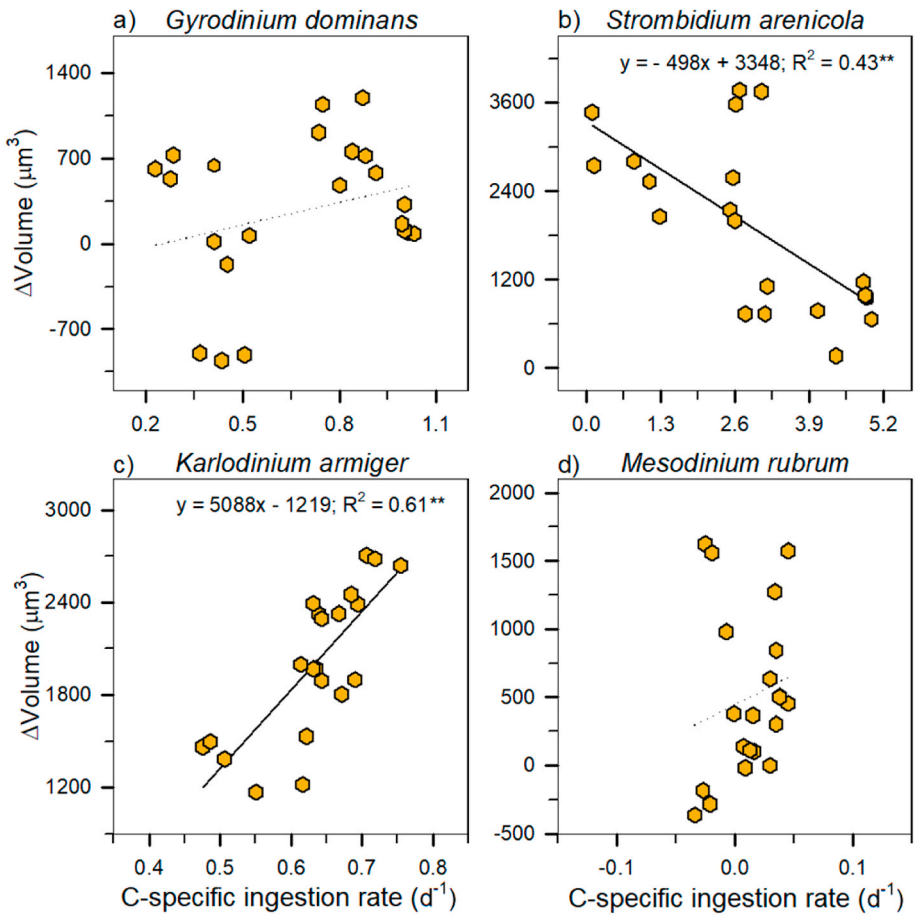

Fig. 4. Linear regression models between C-specific ingestion and changes in predator's volumes (µm^3). Non-significant regressions ($P > 0.05$) are depicted with a dotted line, whereas significant regressions are displayed with a solid line (** implies $P < 0.01$).

and 4b). Therefore, it means that i) smaller *S. arenicola* grew faster than larger ones and that ii) smaller cells have higher C-specific ingestion rates. Being a protozooplanktonic grazer, the principal mechanism of C acquisition is through the ingestion of particulate matter. As such, we can conclude that the overall decrease in volume at higher temperatures (Fig. 2d) results from an enhanced cellular division rate, which in turn can only be attained due to higher C-specific ingestion rates. Similarly, *T. amphioxeia* also became smaller due to faster growth rates at higher temperatures. The conclusions for *S. arenicola* and *T. amphioxeia* are supported by the direct calculation of doubling times as ln (2)/µ (cell--specific) for the chosen temperatures (Figs. S3b and d).

On the contrary, species like the dinoflagellate *G. dominans* and the ciliate *M. rubrum* showed a positive regression between ΔVolume and C-specific growth while displaying a non-significant relationship with C-specific ingestion rates (Fig. 3c,f and **4a,d**). Thus, it seems that the smaller cells, observed at higher temperatures (Fig. 2c,f), are due to somatic reasons, i.e., higher temperatures shrink individual cells, although not necessarily as a consequence of higher cell-specific growth rates (Figs. S3c and f). On the other hand, *K. armiger* showed significant positive slopes between ΔVolume vs C-specific growth and C-specific ingestion vs ΔVolume (Figs. 3e and 4c). This means that the variation in volume (not cellular division – see Fig. S3e) can explain changes in growth, and that ingestion is the cause for the enlargement of the predator's cell. Accordingly, at lower temperatures, the only logical conclusion is that *K. armiger* did not digest the ingested cells and did not divide, resulting in a very significant increase in its size (Fig. S5). Hence, we can conclude that the pattern seen in Fig. 2e was a consequence of the effect of temperature on grazing and not directly on *K. armiger*'s volume.

4.3. Temperature effects on physiological rates

According to our Q_{10} coefficients, only protozooplanktonic species are expected to increase their grazing rates in a sudden warming scenario, being the ciliate *S. arenicola* the species benefiting the most, with a Q_{10} of 3.09 (Table 3). In the case of mixoplankton, both species exhibited a value < 1, which indicates that an increase in the ambient temperature will cause a decreased ingestion of particulate food. The magnitude of the effects of temperature on the four grazers agrees with the maximum ingestion rates of their respective functional responses. Indeed, *S. arenicola* consumed as much as 120 *R. salina* predator^{-1} d^{-1} (Ferreira et al., 2021), whereas *M. rubrum* only ate ca. 5 *T. amphioxeia* predator^{-1} d^{-1} (Smith and Hansen, 2007). *G. dominans* and *K. armiger* stand in between the two ciliates, with the protozooplankter eating ca. 20 *R. salina* predator^{-1} d^{-1} (Calbet et al., 2013) and the mixoplankter ca. 10 *R. salina* predator^{-1} d^{-1} (Berge et al., 2008). This correlation could be a consequence of the C requirements for each species and their mechanism of acquisition (i.e., how much phagotrophy contributes to the overall C budget).

Regarding respiration rates, the effect of temperature was also higher in protozooplankton than in mixoplankton, as seen by the higher Q_{10} for this rate in the first group. This result implies that protozooplankters will lose proportionally more C through respiration in a warming scenario than mixoplankters. This is likely a consequence of internal photosynthetic mechanisms in mixoplankton, which often (if not always) prioritise internal over external C sources i.e., the internal recycling of C decreases their overall void of C (Flynn and Mitra, 2009). Conversely, for protozooplankton, grazing is the only source of C acquisition and, therefore, it seems logical to find a correlation between C intake by

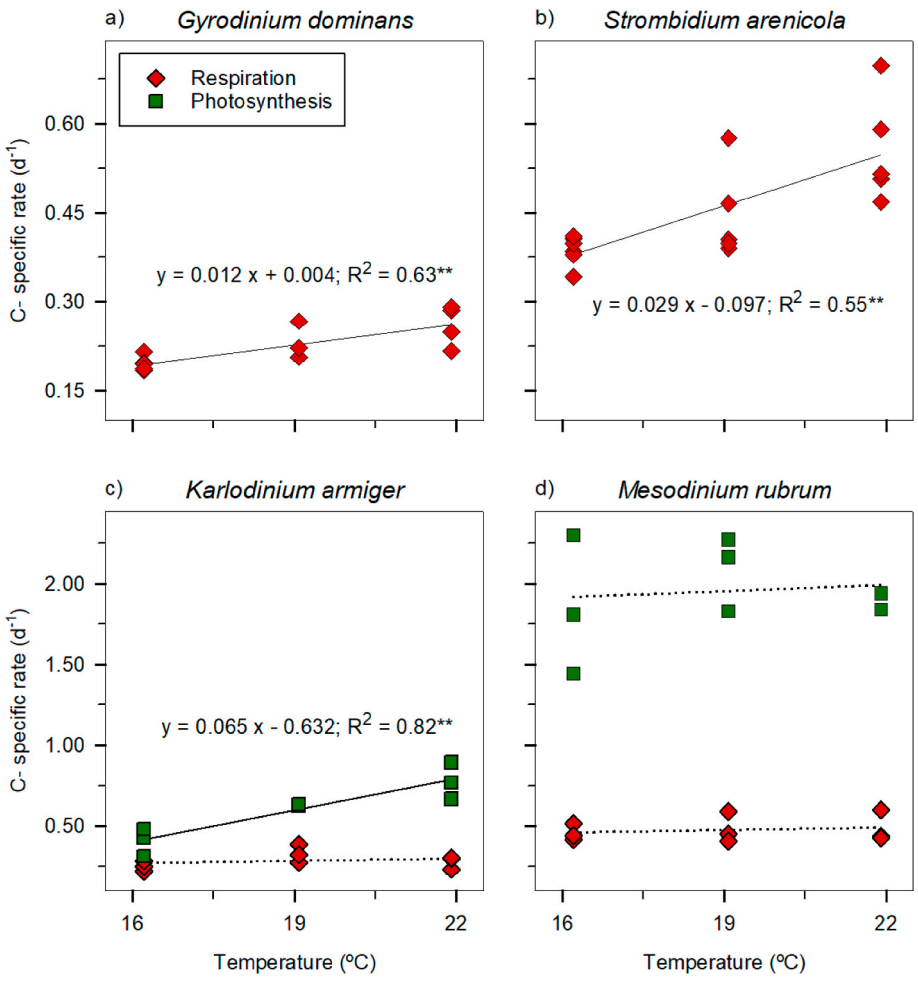

Fig. 5. C-specific respiration (red diamonds) and photosynthetic (green squares) rates for a) *G. dominans*, b) *S. arenicola*, c) *K. armiger*, and d) *M. rubrum* for temperatures between 16.2 and 21.9 °C. Non-significant regressions ($P > 0.05$) are depicted with a dotted line, whereas significant regressions are displayed with a solid line (** implies $P < 0.01$).

Table 3
Q_{10} for every physiological rate ascertained in this study for the predator species. Q_{10} was calculated using Equation (4) (Vaquer-Sunyer et al., 2010)
NA = not applicable.

Species	Growth	Grazing	Respiration	Photosynthesis
Gyrodinium dominans	2.01	2.66	1.67	NA
Strombidium arenicola	1.34	3.09	1.85	NA
Karlodinium armiger	0.80	0.88	1.19	3.16
Mesodinium rubrum	0.92	0.33	1.10	1.11

feeding and C losses due to respiration (as both parameters are integrated into an organism's C budget). It has been reported that residual photosynthesis may occur in protozooplankton due to the presence of algae food in vacuoles (Ferreira et al., 2021; Tarangkoon and Hansen, 2011). Still, in our experiment, all predators were allowed to deplete their co-existent prey on the night before the experiment. Thus, even though photosynthesis was not ruled out as a hypothetical activity in protozooplankton, the lack of prey in the respiration/photosynthesis experiment minimised this potential problem. In addition, respiration rates are typically higher in the presence of food than in its absence (Calbet et al., 2022). In any case, O_{Light} for protozooplankton resulted in negative values, i.e., oxygen consumption during the hours of light. These results were typically slightly lower (on average ca. 5.3% lower) than those in the dark incubations (O_{Dark}), although differences were never statistically significant (Student's t-test, $P > 0.05$ on all cases) and, therefore, dark and light bottles were considered as replicates for the measurement of respiration rates in protozooplankton.

One interesting outcome of our experiments comes from the analysis of photosynthesis in both *K. armiger* and *M. rubrum*, in particular, in light of the Q_{10} coefficients for growth. It seems that the ciliate, whose mode of nutrition is primarily autotrophic (Smith and Hansen, 2007), might not benefit much from a sudden increase of temperature (Q_{10} for photosynthesis ca. 1.11 – Table 3), as predicted by the MTE for autotrophic processes (Brown et al., 2004). On the other hand, *K. armiger*, increased its photosynthetic rate by ca. 1.91 times in less than 6 °C, which resulted in a very high Q_{10} for this process in the dinoflagellate (ca. 3.16 – Table 3). Nevertheless, these increased photosynthetic rates were incapable of sustaining the growth of both predators as temperature rises (Q_{10} for growth is < 1), which suggests that grazing plays an important part in the overall metabolism of these organisms (Q_{10} for grazing <1 for both species). Unsurprisingly, a severely reduced grazing in *M. rubrum* ($Q_{10} = 0.33$) had a lower effect on growth ($Q_{10} = 0.92$) than the one demonstrated by *K. armiger* with a smaller reduction in grazing (Q_{10} for grazing = 0.88; Q_{10} for growth = 0.80). This is likely entirely dependent on their specific reliance on auto/heterotrophic mechanisms of C acquisition, as the ciliate is primarily autotrophic and the dinoflagellate is a voracious feeder (Berge and Hansen, 2016; Smith and Hansen, 2007).

Considering all four physiological rates measured in this study, we can attempt to place these organisms within the MTE framework. A critical aspect that is conserved in both mixoplanktonic predators is that

photosynthesis is the rate that benefits the most from temperature (although the differences across rates are minor in *M. rubrum*). In addition, grazing was always hindered in a sudden warming scenario in both species (seen by a $Q_{10} < 1$ – Table 3). Moreover, digestion rates depend on the ambient temperature but vary similarly in mixoplanktonic and protozooplanktonic grazers (Fenchel, 1975; Li et al., 2001). This particular combination of factors suggests that both mixoplanktonic species (irrespective of their taxonomic group) increase their auto/heterotrophic ratio at higher temperatures, as opposed to the predictions of the MTE for strict autotrophic and heterotrophic organisms (Brown et al., 2004) and to some experimental studies as well (Cabrerizo et al., 2019; Wilken et al., 2013). Nevertheless, our results are not the first to report an atypical behaviour of mixoplankton in light of the MTE projections. For example, a direct measurement of the contribution of grazing to the total metabolic budget in the bacterivore mixoplankter *Dinobryon sociale* resulted in a higher contribution of phototrophy at higher temperatures (Princiotta et al., 2016). Similarly, González-Olalla et al. (2019) assessed the effect of temperature on two bacterivores and concluded that warmer temperatures shifted the overall metabolism towards an increased phototrophy in both species. Also, Ok et al. (2019) studied the mixoplanktonic dinoflagellate *Takayama helix* (same family as *K. armiger*) and noticed increased growth rates paired with insignificant changes in ingestion rates in a wide temperature range. Lim et al. (2019) and Kang et al. (2020) noticed the same pattern in the mixoplanktonic dinoflagellates *Alexandrium pohangense* and *Yihiella yeosuensis*, respectively. Altogether, the results from these latter three works hint at a possibly higher phototrophic contribution to the overall metabolism in these dinoflagellate species, although this variable was not directly measured in their study.

Still, our results do not question prior estimations of *Ea* in phototrophs and heterotrophs based on growth rates (e.g., Rose and Caron, 2007), as the average Q_{10} for protozooplanktonic growth was more than twice that of mixoplankton (which was lower than 1 on both cases). Nevertheless, recent evidence demonstrated that the *Ea* values for growth are widely variable among different taxonomic groups (Chen and Laws, 2017). In addition, the nutritional plasticity of mixoplankton has been pointed as a possible source of error between theoretical and observed *Ea* in microplankton (Wang et al., 2019). Therefore, as our results support an increased phototrophy in mixoplankton at higher temperatures, we contribute to the body of literature that deviates mixoplankton from the MTE. This conclusion means that such a change in nutritional strategies will likely impact biogeochemical cycles and reinforces the need to integrate mixoplankton in current ecosystem models (Wilken et al., 2018).

4.4. Final remarks

It is important to stress the laboratory nature of this study and the inherent adaptation to a constant temperature in the species (and strains) considered. In spite of being a perfectly natural approach to study microplanktonic communities for logistical reasons (Flynn et al., 2019), field communities likely experience temperature oscillations within a day (e.g., Olivares et al., 2022). These natural diel variations may decrease the overall effect of temperature on the physiological rates assessed in our study since the effects of adaptation to a specific set of abiotic conditions is mostly absent in the field. Indeed, future studies should also address the multigenerational response to temperature changes since a general (and gradual) increase in the oceanic temperature is also expected due to climate change (Xiao et al., 2019). Accordingly, adaptation will likely be reflected in the biological rates and overall metabolism, meaning that these changes must also be incorporated in future modelling predictions (Calbet and Saiz, 2022). In this regard, evidence from evolutionary studies suggests that, despite having a stronger temperature dependence, heterotrophic processes are balanced with autotrophic ones with passing generations, which culminates with higher C fixation rates in a future warming scenario (Barton et al., 2020; Padfield et al., 2016). Nevertheless, the data presented in this work should assist in comprehending the effect of climate change in marine protistan communities regarding short-term temperature events such as marine heatwaves. Finally, our study contributes to the correct placement of mixoplankton within the MTE, which may be crucial for the accurate projection of climate change in the future.

Author contributions

All authors conceptualized the experiments. G.D.F. and A.G. prepared the cultures and conducted the experiments. A.C. and E.S. provided material, facilities and assistance to the development of the experiments. G.D.F., A.C., and E.S. analysed the data. G.D.F. and A.C. prepared the original draft manuscript. All authors read, contributed, and approved the final version of the manuscript thus justifying all authorships.

Declaration of competing interest

The authors declare that they have no known competing financial interests or personal relationships that could have appeared to influence the work reported in this paper.

Acknowledgements

This project has received funding from the European Union's Horizon 2020 research and innovation programme under the Marie Skłodowska-Curie grant agreement No. 766327. This document reflects only the author's view; the REA and the European Commission are not responsible for any use that may be made of the information it contains. Thanks for financial support are also due to the ERASMUS + traineeship program and to the Grants CTM 2017–84288-R and PID 2020-118645RB-I00 funded by MCIN/AEI Spain/10.13039/501100011033 and by "FEDER Una manera de hacer Europa". This work is a contribution of the Marine Zooplankton Ecology Group (2017 SGR 87) with the institutional support of the 'Severo Ochoa Centre of Excellence' accreditation (CEX 2019-000928-S). We want to thank all the people from the lab involved in keeping the cultures alive during all the months the experiments lasted, particularly during the restrictive and dangerous confinement period of the pandemic COVID-19. The authors declare no competing interests.

Appendix A. Supplementary data

Supplementary data to this article can be found online at https://doi.org/10.1016/j.marenvres.2022.105693.

References

Almeda, R., Alcaraz, M., Calbet, A., Saiz, E., 2011. Metabolic rates and carbon budget of early developmental stages of the marine cyclopoid copepod *Oithona davisae*. Limnol. Oceanogr. 56, 403–414.

Angert, A.L., Sheth, S.N., Paul, J.R., 2011. Incorporating population-level variation in thermal performance into predictions of geographic range shifts. Integr. Comp. Biol. 51, 733–750.

Angilletta Jr., M.J., Angilletta, M.J., 2009. Thermal Adaptation: a Theoretical and Empirical Synthesis. Oxford University Press, New York.

Barton, S., Jenkins, J., Buckling, A., Schaum, C.-E., Smirnoff, N., Raven, J.A., Yvon-Durocher, G., 2020. Evolutionary temperature compensation of carbon fixation in marine phytoplankton. Ecol. Lett. 23, 722–733.

Berge, T., Hansen, P.J., 2016. Role of the chloroplasts in the predatory dinoflagellate *Karlodinium armiger*. Mar. Ecol. Prog. Ser. 549, 41–54.

Berge, T., Hansen, P.J., Moestrup, Ø., 2008. Prey size spectrum and bioenergetics of the mixotrophic dinoflagellate *Karlodinium armiger*. Aquat. Microb. Ecol. 50, 289–299.

Brown, J.H., Gillooly, J.F., Allen, A.P., Savage, V.M., West, G.B., 2004. Toward a metabolic theory of ecology. Ecology 85, 1771–1789.

Cabrerizo, M.J., González-Olalla, J.M., Hinojosa-López, V.J., Peralta-Cornejo, F.J., Carrillo, P., 2019. A shifting balance: responses of mixotrophic marine algae to cooling and warming under UVR. New Phytol. 221, 1317–1327.

Calbet, A., Isari, S., Martínez, R.A., Saiz, E., Garrido, S., Peters, J., Borrat, R.M., Alcaraz, M., 2013. Adaptations to feast and famine in different strains of the marine

heterotrophic dinoflagellates *Gyrodinium dominans* and *Oxyrrhis marina*. Mar. Ecol. Prog. Ser. 483, 67–84.
Calbet, A., Martínez, R.A., Saiz, E., Alcaraz, M., 2022. Effects of temperature on the bioenergetics of the marine protozoans *Gyrodinium dominans* and *Oxyrrhis marina*. Front. Mar. Sci. 9, 901096.
Calbet, A., Saiz, E., 2022. Thermal acclimation and adaptation in marine protozooplankton and mixoplankton. Front. Microbiol. 13, 832810.
Caperon, J., Schell, D., Hirota, J., Laws, E., 1979. Ammonium excretion rates in Kaneohe Bay, Hawaii, measured by a 15N isotope dilution technique. Mar. Biol. 54, 33–40.
Chakravarti, L.J., Beltran, V.H., van Oppen, M.J.H., 2017. Rapid thermal adaptation in photosymbionts of reef-building corals. Global Change Biol. 23, 4675–4688.
Chen, B., Laws, E.A., 2017. Is there a difference of temperature sensitivity between marine phytoplankton and heterotrophs? Limnol. Oceanogr. 62, 806–817.
Daufresne, M., Lengfellner, K., Sommer, U., 2009. Global warming benefits the small in aquatic ecosystems. Proc. Natl. Acad. Sci. USA 106, 12788–12793.
Eppley, R.W., 1972. Temperature and phytoplankton growth in the sea. Fish. Bull. 70, 1063–1085.
Fenchel, T., 1975. The quantitative importance of the benthic microfauna of an arctic tundra pond. Hydrobiologia 46, 445–464.
Ferreira, G.D., Calbet, A., 2020. Caveats on the use of rotenone to estimate mixotrophic grazing in the oceans. Sci. Rep. 10, 3899.
Ferreira, G.D., Romano, F., Medić, N., Pitta, P., Hansen, P.J., Flynn, K.J., Mitra, A., Calbet, A., 2021. Mixoplankton interferences in dilution grazing experiments. Sci. Rep. 11, 23849.
Fiorendino, J.M., Smith, J.L., Campbell, L., 2020. Growth response of *Dinophysis, Mesodinium*, and *Teleaulax* cultures to temperature, irradiance, and salinity. Harmful Algae 98, 101896.
Flynn, K.J., Mitra, A., 2009. Building the "perfect beast": modelling mixotrophic plankton. J. Plankton Res. 31, 965–992.
Flynn, K.J., Mitra, A., Anestis, K., Anschütz, A.A., Calbet, A., Ferreira, G.D., Gypens, N., Hansen, P.J., John, U., Martin, J.L., Mansour, J.S., Maselli, M., Medić, N., Norlin, A., Not, F., Pitta, P., Romano, F., Saiz, E., Schneider, L.K., Stolte, W., Traboni, C., 2019. Mixotrophic protists and a new paradigm for marine ecology: where does plankton research go now? J. Plankton Res. 41, 375–391.
Franzè, G., Menden-Deuer, S., 2020. Common temperature-growth dependency and acclimation response in three herbivorous protists. Mar. Ecol. Prog. Ser. 634, 1–13.
Frost, B.W., 1972. Effects of size and concentration of food particles on the feeding behavior of the marine planktonic copepod *Calanus pacificus*. Limnol. Oceanogr. 17, 805–815.
Gaillard, S., Charrier, A., Malo, F., Carpentier, L., Bougaran, G., Hégaret, H., Réveillon, D., Hess, P., Séchet, V., 2020. Combined effects of temperature, irradiance, and pH on *Teleaulax amphioxeia* (Cryptophyceae) physiology and feeding ratio for its predator *Mesodinium rubrum* (Ciliophora). J. Phycol. n/a.
Gao, H., Hua, C., Tong, M., 2018. Impact of *Dinophysis acuminata* feeding *Mesodinium rubrum* on nutrient dynamics and bacterial composition in a microcosm. Toxins 10, 443.
González-Olalla, J.M., Medina-Sánchez, J.M., Carrillo, P., 2019. Mixotrophic trade-off under warming and UVR in a marine and a freshwater alga. J. Phycol. 55, 1028–1040.
Guillard, R.R.L., 1975. Culture of phytoplankton for feeding marine invertebrates. In: Smith, W.L., Chanley, M.H. (Eds.), Culture of Marine Invertebrate Animals. Plenum Press, New York, NY, pp. 29–60.
Hammer, A., Schumann, R., Schubert, H., 2002. Light and temperature acclimation of *Rhodomonas salina* (Cryptophyceae): photosynthetic performance. Aquat. Microb. Ecol. 29, 287–296.
Heinbokel, J.F., 1978. Studies on the functional role of tintinnids in the Southern California Bight. I. Grazing and growth rates in laboratory cultures. Mar. Biol. 47, 177–189.
Hochachka, P.W., Somero, G.N., 2002. Biochemical Adaptation: Mechanism and Process in Physiological Evolution. Oxford University Press, New York.
Kang, H.C., Jeong, H.J., Lim, A.S., Ok, J.H., You, J.H., Park, S.A., Lee, S.Y., Eom, S.H., 2020. Effects of temperature on the growth and ingestion rates of the newly described mixotrophic dinoflagellate *Yihiella yeosuensis* and its two optimal prey species. ALGAE 35, 263–275.
Kiørboe, T., MacKenzie, B., 1995. Turbulence-enhanced prey encounter rates in larval fish: effects of spatial scale, larval behaviour and size. J. Plankton Res. 17, 2319–2331.
Leles, S.G., Mitra, A., Flynn, K.J., Tillmann, U., Stoecker, D., Jeong, H.J., Burkholder, J., Hansen, P.J., Caron, D.A., Glibert, P.M., 2019. Sampling bias misrepresents the biogeographical significance of constitutive mixotrophs across global oceans. Global Ecol. Biogeogr. 28, 418–428.
Lemos, M.F.L., Soares, A.M.V.M., Correia, A.C., Esteves, A.C., 2010. Proteins in ecotoxicology – how, why and why not? Proteomics 10, 873–887.
Li, A., Stoecker, D.K., Coats, D.W., 2001. Use of the 'food vacuole content' method to estimate grazing by the mixotrophic dinoflagellate *Gyrodinium galatheanum* on cryptophytes. J. Plankton Res. 23, 303–318.
Lim, A.S., Jeong, H.J., Ok, J.H., You, J.H., Kang, H.C., Kim, S.J., 2019. Effects of light intensity and temperature on growth and ingestion rates of the mixotrophic dinoflagellate *Alexandrium pohangense*. Mar. Biol. 166, 98.
Lin, C.-H., Flynn, K.J., Mitra, A., Glibert, P.M., 2018. Simulating effects of variable stoichiometry and temperature on mixotrophy in the harmful dinoflagellate *Karlodinium veneficum*. Front. Mar. Sci. 5, 320.
Mitra, A., Flynn, K.J., Burkholder, J.M., Berge, T., Calbet, A., Raven, J.A., Granéli, E., Glibert, P.M., Hansen, P.J., Stoecker, D.K., Thingstad, F., Tillmann, U., Våge, S., Wilken, S., Zubkov, M.V., 2014. The role of mixotrophic protists in the biological carbon pump. Biogeosciences 11, 995–1005.
Mitra, A., Flynn, K.J., Tillmann, U., Raven, J.A., Caron, D., Stoecker, D.K., Not, F., Hansen, P.J., Hallegraeff, G., Sanders, R.W., Wilken, S., McManus, G., Johnson, M., Pitta, P., Våge, S., Berge, T., Calbet, A., Thingstad, F., Jeong, H.J., Burkholder, J., Glibert, P.M., Granéli, E., Lundgren, V., 2016. Defining planktonic protist functional groups on mechanisms for energy and nutrient acquisition: incorporation of diverse mixotrophic strategies. Protist 167, 106–120.
Montagnes, D.J.S., Morgan, G., Bissinger, J.E., Atkinson, D., Weisse, T., 2008. Short-term temperature change may impact freshwater carbon flux: a microbial perspective. Global Change Biol. 14, 2823–2838.
Ok, J.H., Jeong, H.J., Lim, A.S., You, J.H., Kang, H.C., Kim, S.J., Lee, S.Y., 2019. Effects of light and temperature on the growth of *Takayama helix* (Dinophyceae): mixotrophy as a survival strategy against photoinhibition. J. Phycol. 55, 1181–1195.
Olivares, M., Calbet, A., Saiz, E., 2022. The neritic marine copepod *Centropages typicus* does not suffer physiological costs from diel temperature fluctuations associated with its vertical migration. Aquat. Sci. 84, 9.
Oliver, E.C.J., Burrows, M.T., Donat, M.G., Gupta, A.S., Alexander, L.V., Perkins-Kirkpatrick, S.E., Benthuysen, J.A., Hobday, A.J., Holbrook, N.J., Moore, P.J., Thomsen, M.S., Wernberg, T., Smale, D.A., 2019. Projected marine heatwaves in the 21st Century and the potential for ecological impact. Front. Mar. Sci. 6, 734.
Padfield, D., Yvon-Durocher, G., Buckling, A., Jennings, S., Yvon-Durocher, G., 2016. Rapid evolution of metabolic traits explains thermal adaptation in phytoplankton. Ecol. Lett. 19, 133–142.
Pasciak, W.J., Gavis, J., 1974. Transport limitation of nutrient uptake in phytoplankton. Limnol. Oceanogr. 19, 881–888.
Princiotta, S.D., Smith, B.T., Sanders, R.W., 2016. Temperature-dependent phagotrophy and phototrophy in a mixotrophic chrysophyte. J. Phycol. 52, 432–440.
Regaudie-de-Gioux, A., Duarte, C.M., 2012. Temperature dependence of planktonic metabolism in the ocean. Global Biogeochem. Cycles 26.
Rose, J.M., Caron, D.A., 2007. Does low temperature constrain the growth rates of heterotrophic protists? Evidence and implications for algal blooms in cold waters. Limnol. Oceanogr. 52, 886–895.
Salles, R., Mattos, P., Iorgulescu, A.-M.D., Bezerra, E., Lima, L., Ogasawara, E., 2016. Evaluating temporal aggregation for predicting the sea surface temperature of the Atlantic Ocean. Ecol. Inf. 36, 94–105.
Schindelin, J., Arganda-Carreras, I., Frise, E., Kaynig, V., Longair, M., Pietzsch, T., Preibisch, S., Rueden, C., Saalfeld, S., Schmid, B., 2012. Fiji: an open-source platform for biological-image analysis. Nat. Methods 9, 676.
Schulte, P.M., Healy, T.M., Fangue, N.A., 2011. Thermal performance curves, phenotypic plasticity, and the time scales of temperature exposure. Integr. Comp. Biol. 51, 691–702.
Sheridan, J.A., Bickford, D., 2011. Shrinking body size as an ecological response to climate change. Nat. Clim. Change 1, 401–406.
Smith, M., Hansen, P.J., 2007. Interaction between *Mesodinium rubrum* and its prey: importance of prey concentration, irradiance and pH. Mar. Ecol. Prog. Ser. 338, 61–70.
Tarangkoon, W., Hansen, P.J., 2011. Prey selection, ingestion and growth responses of the common marine ciliate *Mesodinium pulex* in the light and in the dark. Aquat. Microb. Ecol. 62, 25–38.
Traboni, C., Calbet, A., Saiz, E., 2020. Effects of prey trophic mode on the gross-growth efficiency of marine copepods: the case of mixoplankton. Sci. Rep. 10, 12259.
Vaquer-Sunyer, R., Duarte, C.M., Santiago, R., Wassmann, P., Reigstad, M., 2010. Experimental evaluation of planktonic respiration response to warming in the European Arctic Sector. Polar Biol. 33, 1661–1671.
Vidyarathna, N.K., Papke, E., Coyne, K.J., Cohen, J.H., Warner, M.E., 2020. Functional trait thermal acclimation differs across three species of mid-Atlantic harmful algae. Harmful Algae 94, 101804.
Wang, Q., Lyu, Z., Omar, S., Cornell, S., Yang, Z., Montagnes, D.J.S., 2019. Predicting temperature impacts on aquatic productivity: questioning the metabolic theory of ecology's "canonical" activation energies. Limnol. Oceanogr. 64, 1172–1185.
Wielgat-Rychert, M., Rychert, K., Witek, Z., Zalewski, M., 2017. Calculation of the photosynthetic quotient (PQ) in the gulf of gdańsk (southern baltic). Balt. Coast. Zone 21, 51–60.
Wilken, S., Huisman, J., Naus-Wiezer, S., Van Donk, E., 2013. Mixotrophic organisms become more heterotrophic with rising temperature. Ecol. Lett. 16, 225–233.
Wilken, S., Soares, M., Urrutia-Cordero, P., Ratcovich, J., Ekvall, M.K., Van Donk, E., Hansson, L.A., 2018. Primary producers or consumers? Increasing phytoplankton bacterivory along a gradient of lake warming and browning. Limnol. Oceanogr. 63, S142–S155.
Williams, P.J.I.B., del Giorgio, P.A., 2005. Respiration in aquatic ecosystems: history and background. In: del Giorgio, P.A., Williams, P.J.I.B. (Eds.), Respiration in Aquatic Ecosystems. Oxford University Press, Oxford University Press Inc., New York, pp. 1–17.
Xiao, C., Chen, N., Hu, C., Wang, K., Gong, J., Chen, Z., 2019. Short and mid-term sea surface temperature prediction using time-series satellite data and LSTM-AdaBoost combination approach. Remote Sens. Environ. 233, 111358.